Impulse excitation of piezoelectric bimorphs for energy harvesting: a dimensionless model

Michele Pozzi

School of Mechanical and Systems Engineering, Newcastle University, Newcastle upon Tyne, NE1 7RU, UK

E-mail: michele.pozzi@newcastle.ac.uk

Abstract. Energy harvesting (EH) is a multidisciplinary research area, involving physics, materials science and engineering, with the objective of providing renewable sources of power sufficient to operate targeted low-power applications. Piezoelectric transducers are often used for inertial vibrational as well as direct-excitation EH. However, due to the stiffness of the most common material (PZT), compact and light-weight harvesters have high resonant frequencies, making them inefficient at extracting low frequency power from the environment. The technique of frequency up-conversion, in the form of either plucking or impulse excitation, aims to bridge this frequency gap. In this paper, the technique is modelled analytically with focus on impulse excitation via impact or shock. An analytical model is developed in a standard way starting from the Euler-Bernoulli beam equations adapted to a piezoelectric bimorph. A set of dimensionless variables and parameters is defined and a system of differential equations derived. Here the system is solved numerically for a wide range of the two group parameters present, covering piezoelectric coupling strength between PVDF and PMN-PT. One major result is that the strength of the coupling strongly affects the time-scale of the process, but has only a minor effect on the total energy converted. The model can be readily adapted to different excitation profiles.

Keywords: Energy Harvesting, impact excitation, impulse excitation, frequency up-conversion, piezoelectric bimorph, dimensionless model.

1. Introduction

Energy harvesting (EH) has been a hot topic in recent years, attracting interest from mechanical, electronic and systems engineers, businesses, material scientists and physicists. With the purpose of scavenging energy from the environment for the most diverse range of applications (sensing, monitoring, automation, healthcare, ...) a host of physical phenomena are investigated and exploited.

The high stiffness of piezoelectric ceramics such as PZT (the most commonly used piezoelectric material) causes difficulties in the design of EHs efficiently tuned to the environment, where the vibration spectrum has typically lower power content at high frequencies. For this reason, the piezoelectric transducer normally favoured in EH is the PZT bimorph in a cantilevered beam configuration, often with a tip mass to further reduce the resonance frequency. A drawback is that the high fundamental frequency intrinsic to piezoelectric transducers is sacrificed, even though it is always desirable as higher frequencies mean the potential of higher power generation. The frequency mismatch issue is even more severe within the scope of human-based energy harvesting, given that human motions are intrinsically slow.

It is therefore clear the need for a technique capable of bridging between the high-frequency response of piezoelectric bimorphs and the low-frequency input that is most often available in the environment and on the human body. This up-frequency conversion can be achieved in two distinct ways. The plucking or "pizzicato" technique [1, 2] is based on elastically deforming the bimorph with a plectrum and permitting free vibrations upon release; in the latter phase, the stored elastic energy is converted into electrical energy. The other embodiment of frequency up-conversion is impulse excitation [3], where momentum is transferred to the bimorph, usually via impact with a projectile. It is worthwhile to compare and contrast these two techniques. In plucking excitation, the piezoelectric devices are slowly deformed and then released; mathematically, the system's initial conditions feature a non-zero displacement; the principle is equivalent to the plucking of chords in a guitar (or a violin when the *pizzicato* technique is used). From the physical point of view, impact involves the transfer of momentum; mathematically, the system's initial conditions have non-zero velocity; the principle is similar to hammers striking the wires in a piano.

Frequency up-conversion techniques have been applied to situations where environmental vibrations are at much lower frequency than the transducers' natural frequency. For example, Kulah and Najafi, [4] have developed a micro-scale electromagnetic harvester where the low-frequency vibration of a suspended magnet excites the high frequency vibration of a number of coil-carrying cantilevers placed around it. Frequency up-conversion techniques can also be applied to scavenge energy from slow rotary motions [5, 6], from oceanic waves [7] and to wearable energy harvesters [8]. Some examples of impact excitation are a hand-held device by Renaud et al. [9] and a smaller device by Cavallier et al. [10]; more recently other authors have applied the technique in the microscale with piezoelectric [11] and electrostatic transduction [12].

Gu and Livermore [13] presented a self-tuning EH that produces periodic impacts on a piezoelectric beam when installed on a disc rotating in a vertical plane; the work also offers basic modelling for the optimisation of some design parameters.

Although the principle behind the impulse technique of frequency up-conversion is rather simple, it is important to model the process to understand its potential and its dominating features as an energy harvesting technique, to select the most appropriate piezoelectric material and to establish the effects of different types of impact. In the design of an impulse excited EH it is also important to determine the optimal impact frequency: a dynamic, time-dependent description of the cantilever's movement permits to decide when sufficient energy has been extracted from that event and it is more beneficial to produce a new impact rather than wait for a full conversion of the imparted energy. A detailed modelling of impact-excitation has been presented by Jacquelin et al. [14] and applied to the device prototyped by Renaud et al. [9]. Renaud's harvester features two piezoelectric monomorphs excited by impacts of a sliding mass which travels between the two when the whole device is vigorously shaken side to side. Jacquelin's model describes the explicit dynamics of the impact, including Hertzian contact forces, the motion of the mass and the vibration of the beam. Jacquelin studied the effect of some individual parameters on the average power produced with a fixed external excitation.

The present paper differs from and complements Jacquelin's work, as focus is on the transducer itself and the role played by the piezoelectric coupling and the external resistor. Whereas Jacquelin et al. applied their method to a specific harvester and optimised its design parameters, here we try to draw as widely applicable conclusions as possible – for instance, the beam's size remains unspecified as the model is dimensionless. The optimisation of the impact conditions (mass and velocity of projectile, hardness of the contacting surfaces, etc.) is a very complex problem, in part addressed by Jacquelin. In the present paper, there is no attempt to investigate the details of the impact itself, rather it is assumed that the contact force versus time is approximated by a bell-shaped curve (specifically, a Gaussian), which is a good approximation even when the impact conditions vary significantly, for example going from simple impact to multiple impacts [15]. The present work offers guidelines to the design of efficient and cost effective impulse-excited EHs that can be immediately applied in their qualitative content and whose quantitative benefits can be calculated once the dimensionless results presented are particularised for the problem in hand.

2. Dimensionless model

In this section, the classical treatment of a vibrating clamped-free beam is adapted to a piezoelectric bimorph; for more details on the Euler-Bernoulli beam-related derivations, the reader is referred to a book on vibrations such as [16]. More details on the derivations for a piezoelectric beam can be found in [17].

Indicating with the attribute tilde ($\tilde{}$) variables and parameters which have

dimensions, the governing differential equation of a piezoelectrically active Euler-Bernoulli beam (figure 1) is:

$$\frac{\partial^2 \tilde{M}_{mech}}{\partial \tilde{x}^2} + \frac{\partial^2 \tilde{M}_{el}}{\partial \tilde{x}^2} + \tilde{c}_a \frac{\partial \tilde{u}}{\partial \tilde{t}} + \tilde{\rho}\tilde{w}\tilde{h}\frac{\partial^2 \tilde{u}}{\partial \tilde{t}^2} = \tilde{f}(\tilde{x}, \tilde{t}) \tag{1}$$

where $\tilde{c}_a$ is the coefficient of viscous damping (e.g. air damping), $\tilde{\rho}$ is the average volumetric mass density, $\tilde{h}$ is the total thickness of the beam, $\tilde{w}$ is its width and $\tilde{f}(\tilde{x}, \tilde{t})$ is an external forcing function. The definition of coordinates and other geometrical parameters used later are indicated in figure 1. As indicated in (1), the bending moment is made of two terms, of mechanical and electrical origin respectively. The mechanical term is simply given by:

$$\tilde{M}_{mech} = \tilde{B}\frac{\partial^2 \tilde{u}}{\partial \tilde{x}^2} \tag{2}$$

Considering the sandwich-like structure, the bending stiffness can be written:

$$\tilde{B} = 2\tilde{Y}_{pz}\tilde{I}_{pz} + \tilde{Y}_{ms}\tilde{I}_{ms} = \tilde{Y}_{pz}\tilde{w}\tilde{h}^3\left[\frac{h_r^3}{6} + \frac{(1-h_r)^2 h_r}{2} + \frac{\tilde{Y}_{ms}}{\tilde{Y}_{pz}}\frac{(1-2h_r)^3}{12}\right]$$

here the pz and ms subscripts stand for piezoelectric layer(s) and internal metal substrate, respectively; Y is the Young's modulus in the x or y direction, which are equivalent for a piezoelectric ceramic poled along the z axis; $\tilde{I}$ is the second moment of an area; $\tilde{w}$ is the width of the bimorph; $\tilde{h} = 2\tilde{h}_{pz} + \tilde{h}_{ms}$ and $h_r \overset{\text{def}}{=} \tilde{h}_{pz}/\tilde{h}$.

At this point, it is convenient to introduce the parameter c_B , which contains the elastic and geometrical properties of the bimorph:

$$c_B \overset{\text{def}}{=} \frac{\tilde{B}}{\tilde{Y}_{pz}\tilde{w}\tilde{h}^3} = \frac{h_r^3}{6} + \frac{(1-h_r)^2 h_r}{2} + \frac{\tilde{Y}_{ms}}{\tilde{Y}_{pz}}\frac{(1-2h_r)^3}{12} \tag{3}$$

so that (2) can be re-written:

$$\tilde{M}_{mech} = c_B\, \tilde{Y}_{pz}\, \tilde{w}\, \tilde{h}^3\, \frac{\partial^2 \tilde{u}}{\partial \tilde{x}^2} \tag{4}$$

The inverse piezoelectric effect introduces a bending moment of electrical origin. This can be derived from the constitutive equation of piezoelectricity $S_1 = s_{11}^E T_1 + d_{31}E_3$ that takes this form because of the position of the electrodes ($E_1 = E_2 = 0$) and the geometry of the beam, which permits to neglect all stresses except the longitudinal tensile [18]. This equation can be manipulated to give the stress T as a function of the applied electric field E and the strain S (the dependence on spatial and temporal coordinates is omitted for compactness):

$$T_1 = Y_{pz}S_1 - d_{31}Y_{pz}E_3 \tag{5}$$

Ignoring its first term as it is already taken care of by (2), the second term gives:

$$\tilde{M}_{el} = 2\int \tilde{T}\ \tilde{z}\ d\tilde{a}\ =\ 2\int_{\tilde{h}_{ms}/2}^{\tilde{h}/2} \tilde{d}_{31}\tilde{Y}_{pz}\frac{\tilde{V}}{2\tilde{h}_{pz}}\tilde{z}(\tilde{w}d\tilde{z}) = \frac{1}{2}\tilde{d}_{31}\tilde{Y}_{pz}\tilde{w}\tilde{h}(1-h_r)\tilde{V} \tag{6}$$

where we have used the relationship between electric field and voltage $\tilde{E}_3 = -\tilde{V}/(2\tilde{h}_{pz})$, which assumes a series bimorph.

Combining equations (1), (4) and (6), the governing equation for a piezoelectrically active beam can be written as:

$$c_B\tilde{Y}_p z\tilde{w}\tilde{h}^3\frac{\partial^4\tilde{u}}{\partial\tilde{x}^4} + \frac{1}{2}\tilde{d}_{31}\tilde{Y}_{pz}\tilde{w}\tilde{h}(1-h_r)\frac{\partial^2\tilde{V}}{\partial\tilde{x}^2} + \tilde{c}_a\frac{\partial\tilde{u}}{\partial\tilde{t}} + \tilde{\rho}\tilde{w}\tilde{h}\frac{\partial^2\tilde{u}}{\partial\tilde{t}^2} = \tilde{f}(\tilde{x},\tilde{t}) \tag{7}$$

In order to derive the corresponding dimensionless equation, a new set of dimensionless variables is needed (see Table 1). These definitions are developed with reference to [19], adapted and extended to include the electrical quantities. After some manipulations, the equation becomes:

$$\frac{1}{k_1^4}\frac{\partial^4 u}{\partial x^4} + 2\zeta\frac{\partial u}{\partial t} + \chi\frac{\partial^2 V}{\partial x^2} + \frac{\partial^2 u}{\partial t^2} = g(x,t) \tag{8}$$

where two new dimensionless coefficients are defined:

$$\zeta \stackrel{\text{def}}{=} \frac{\tilde{\omega}_1\tilde{L}^4}{2k_1^4\tilde{B}}\tilde{c}_a \qquad \chi \stackrel{\text{def}}{=} \frac{(1-h_r)}{2c_B k_1^4 h^2}$$

the following relation is also introduced (see e.g. [19]):

$$\tilde{\omega}_1^2 = \frac{k_1^4 c_B\tilde{Y}_{pz}\tilde{h}^2}{\tilde{\rho}\tilde{L}^4}$$

and the dimensionless forcing is:

$$g(x,t)\ =\ \frac{\tilde{f}(\tilde{x},\tilde{t})\tilde{L}^3}{k_1^4\tilde{B}}.$$

Note that in the equations above, k_1 is the first solution to the frequency equation $1+\cos k\cosh k\ =\ 0$, which applies when the boundary conditions for a cantilevered beam are imposed [16].

Within the scope of this paper, the forcing function $g(x,t)$ must represent a low velocity impact excitation. The exact time-dependence of the force between two impacting bodies depends upon their shape, the materials they are made of, their masses, the relative velocities, their constraints, etc. As this paper is devoted to a generic impact of a cantilevered beam with an almost free projectile, it is sufficient to select a function with these main features: zero before and after contact, sharp rise up to a maximum, corresponding to maximum approach, and subsequent sharp decrease. A common function satisfying these requirements is the Gaussian:

$$g(x,t)\ =\ \frac{J}{\sqrt{2\pi}\,\sigma}\exp\left[-\frac{(t-t_0)^2}{2\sigma^2}\right]\delta(x-x_0) \tag{9}$$

Table 1. Dimensionless variables and parameters (expanded from [19])

Symbol	Description	Relation
L, w, h	length, width, thickness	$\tilde{o} = \tilde{L}o$
u	displacement	$\tilde{u} = \tilde{L}u$
t	time	$\tilde{t} = t/\tilde{\omega_1}$
ρ	volumetric mass density	$\tilde{\rho} = \rho\tilde{B}/(\tilde{L}^6\,\tilde{\omega}^2)$
V	voltage	$\tilde{V} = V\tilde{L}/\tilde{d}_{31}$

governed by the following parameters:

J dimensionless impulse transferred during impact;

σ width of the Gaussian – this can be used to study sharp (small σ) or dull impacts (large σ);

t_0 time of maximum approach. It is assumed that the first contact occurs at $t_0 - 3\sigma$, which was set as $t = 0$ in the following numerical solutions, so that $t_0 = 3\sigma$.

x_0 the point of impact along the beam (using the Dirac δ).

As is well known, when a piezoelectric material is strained it develops an electrical charge, as a consequence of a change in polarisation. This is the direct piezoelectric effect and is still to be included in the model: free charges tend to displace to balance the change in polarisation, but can do so only via the external circuit, whose resistance contributes then to determine the strength of the electric field in the piezoelectric material; this field is connected to the voltage present in (6). So, to take into account the effect of the electrical circuit, we have to relate the voltage to the current, which is the time derivative of the charge Q, which in turn is given by the surface integral of the electric displacement D over the electrode area:

$$\tilde{I}(\tilde{t}) = \frac{d\tilde{Q}(\tilde{t})}{d\tilde{t}} = \frac{d}{d\tilde{t}} \int_0^{\tilde{L}} \tilde{D}_3(\tilde{x}, \tilde{t}) \tilde{w}\, d\tilde{x} \tag{10}$$

where D_3 (the component of the displacement parallel to the poling direction and giving the charge density on the electrodes) is given by another constitutive equation of piezoelectricity $D_3 = d_{3j}T_j + \epsilon_{33}^T E_3$, which in this setting becomes:

$$\tilde{D}_3(\tilde{x}, \tilde{t}) = \tilde{d}_{31}\tilde{Y}_{pz}\tilde{S}_1(\tilde{x}, \tilde{t}) - \epsilon_3^S \frac{\tilde{V}(\tilde{t})}{2\tilde{h}_{pz}} \tag{11}$$

In (11) the spatial and temporal variables are made explicit: whereas D_3 and S_1 depend on both, the voltage is uniform on the surfaces of the piezoelectric material because of the electrodes. Upon substituting (11) into (10), the expression for the current is:

$$\tilde{I}(\tilde{t}) = -\frac{1}{2}\tilde{d}_{31}\tilde{Y}_{pz}\tilde{h}(1 - h_r)\tilde{w} \left| \frac{\partial^2 \tilde{u}}{\partial\tilde{t}\partial\tilde{x}} \right|_0^{\tilde{L}} - \frac{\tilde{w}\tilde{L}\epsilon_3^S}{2\tilde{h}_{pz}} \frac{d\tilde{V}}{d\tilde{t}}$$

Using Ohm's first law for the current through an external resistor of value R and introducing the dimensionless variables from Table 1, the direct piezoelectric effect is described by:

$$\frac{dV}{dt} + \frac{V}{\tau} + \Phi \left| \frac{\partial^2 u}{\partial t \partial x} \right|_0^1 = 0 \tag{12}$$

where two new dimensionless parameters are defined:

$$\begin{aligned} \Phi &\stackrel{\text{def}}{=} k_{31}^2 h_r h^2 (1 - h_r) \epsilon_{33}^T / \epsilon_{33}^S \\ \tau &\stackrel{\text{def}}{=} \epsilon_{33}^S \tilde{R} w \tilde{L} \tilde{\omega}_1 / 2 h_r h \end{aligned} \tag{13}$$

The coupling coefficient has been introduced as $k_{31}^2 = \tilde{d}_{31}^2 \tilde{Y}_{pz} / \epsilon_{33}^T$.

The solution of the system formed by equations (12) and (8) proceeds by separation of variables [17] by setting:

$$u(x,t) = \sum_{n=1}^{\infty} \phi_n(x) q_n(t)$$

Note that the ϕ_n, which must offer an orthonormal base in the functional space $L^2([0,1])$, can be conveniently chosen as is customary for a cantilevered Euler-Bernoulli beam.

If the approximation includes N modes, the system is:

$$\begin{aligned} &\frac{d^2 q_n}{dt^2} + 2\zeta \left(\frac{k_n}{k_1} \right)^4 \frac{dq_n}{dt} + \left(\frac{k_n}{k_1} \right)^4 q_n - \phi_n'(1) \chi V = g(t) \phi_n(x_0) \\ &\frac{dV}{dt} + \frac{V}{\tau} + \Phi \sum_{n=1}^{N} \phi_n'(1) \frac{dq_n}{dt} = 0 \qquad n = 1, 2, ..., N \end{aligned}$$

here k_n is the n^{th} solution to the already mentioned frequency equation: $1 + \cos k \cosh k = 0$; the $\phi_n(x_0)$ multiplier is the result of the internal product of ϕ_n with the Dirac function in $g(x,t)$; the first derivative of the mode shapes in the origin (i.e. $\phi_n'(0)$) has disappeared as it is zero for a beam clamped at the origin.

At this point, it is apparent that a more convenient definition for the dimensionless voltage would be $\hat{V} \stackrel{\text{def}}{=} V/\Phi$ so that the coupling between the two sets of equations is gauged by a single dimensionless parameter:

$$\begin{aligned} &\frac{d^2 q_n}{dt^2} + 2\zeta \left(\frac{k_n}{k_1} \right)^4 \frac{dq_n}{dt} + \left(\frac{k_n}{k_1} \right)^4 q_n - \phi_n'(1) \Gamma \hat{V} = g(t) \phi_n(x_0) \\ &\frac{d\hat{V}}{dt} + \frac{\hat{V}}{\tau} + \sum_{n=1}^{N} \phi_n'(1) \frac{dq_n}{dt} = 0 \qquad n = 1, 2, ..., N \end{aligned} \tag{14}$$

with

$$\Gamma \stackrel{\text{def}}{=} \Phi \chi = \frac{1}{2k_1^4} \cdot \frac{h_r (1 - h_r)^2}{c_B} \cdot \frac{k_{31}^2 \epsilon_{33}^T}{\epsilon_{33}^S} \tag{15}$$

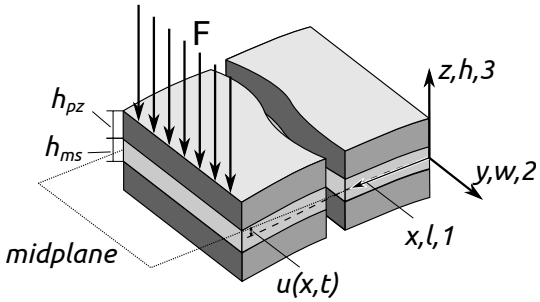

Figure 1. Sketch of the piezoelectric bimorph with relevant dimensions and notations used in the model.

3. Methodology

3.1. Quality factors and design schemes

In this section some quality factors (QFs) are introduced, which are later used to discuss the performance of the EH. The first QF is the cumulative (electrical) energy output of the harvester:

$$E_c(t) = \int_0^t P(t)dt \tag{16}$$

In this expression, the instantaneous power P is always positive, if a purely resistive load is assumed, so that E_c is a monotonic function of time. As the vibration dies down, E_c asymptotically approaches a final value, which will be determined by several factors, including the efficiency with which the impact excitation is converted into mechanical energy, the strength of the electro-mechanical coupling and the damping. The latter two are correlated in the following way: a small coupling implies a long lasting vibration and hence a large loss due to damping, since a fraction of remaining energy is dissipated at every cycle.

For practical purposes, the total energy output is the most important QF if impacts are so sparse that even a slow conversion is complete before the next impact occurs. However, when impacts can be realized with sufficient frequency, it is equally important to minimize the time required to produce the energy output. It is therefore useful to introduce the average power:

$$P_{av}(t) = \frac{E_c(t)}{t} \tag{17}$$

and to study its time evolution.

A typical curve of P_{av} for an impact-excited bimorph (figure 3) is characterized by a steep initial rise, when a large amount of energy is produced by the very ample first vibration cycles, followed by a decrease when most of the energy has already been converted. Between the two regimes is a peak occurring at t_{mx}, which is important to determine the maximum average power the device can produce: in principle, if impacts are repeated with the corresponding frequency $(1/t_{mx})$, the device outputs an average

power equal to the height of the peak, $P_{av}(t_{mx})$. In such operating conditions, a lower overall efficiency can be expected of the device, corrected by the factor:

$$\eta = \frac{E_c(t_{mx})}{E_c(t \to \infty)}$$

Therefore, there are two main design schemes:

(i) maximize E_c – suitable for sparse impacts;

(ii) maximise $P_{av}(t_{mx})$ – suitable for EH that can be designed to produce impacts with frequency $1/t_{mx}$.

In general, scheme 1 will yield higher efficiency but lower average power, whereas scheme 2 will offer the highest average power at the price of reduced efficiency. Operating conditions and output requirements will dictate which design scheme should be used for each application.

3.2. Quality factors from model output

When system (14) is solved numerically, a vector $\hat{V}$ is part of the solution. The purpose of this section is to relate $\hat{V}$ to the instantaneous power, from which descend the QFs introduced in the previous section.

Considering a voltage across a purely resistive load and applying the definitions in Table 1 and equation (13), the electrical power is given by:

$$\tilde{P} = \frac{\tilde{V}^2}{\tilde{R}} = \frac{\tilde{L}^3 \tilde{\omega}_1 \epsilon_3^S w}{2hh_r \tilde{d}_{31}^2} \frac{V^2}{\tau}$$

and the corresponding dimensionless power is:

$$P = \frac{\tilde{P}\tilde{L}}{\tilde{B}\tilde{\omega}_1} = \frac{\tilde{L}^4 \epsilon_3^S w}{2hh_r \tilde{B} \tilde{d}_{31}^2} \frac{V^2}{\tau}$$

Finally, using the definition of c_B and introducing Γ and $\hat{V}$ in the previous expression:

$$P = k_1^4 \, \Gamma \, \hat{V}^2 / \tau.$$

Cumulative energy and average power are derived from this via equations (16) and (17).

3.3. The space of parameters

The system in (14) contains only three groups of parameters: ζ, τ and Γ.

The dissipative damping (air drag, internal material damping, ...) has a minor effect on the overall behaviour of the vibrating beam, hence it was not explored in depth. Instead, ζ was set to a fixed value ($\zeta \approx 4\ 10^{-4}$), calculated starting from the mechanical quality factor of a PZT-5H bimorph. In this paper PVDF is treated only

as a complementary case, but it is worth noting that a piezoelectric polymer will have higher internal damping.

Numerical solutions were calculated for the dimensionless parameter τ in the set $\{\log\tau = -1.7, -1.3, -1, -0.7, -0.3, -0.1, 0, 0.1, 0.3\}$ recognising that whichever value yields the optimal performance, it can be realized for practical devices by tuning the output circuit, a field of research not within the scope of this work.

As for Γ, the second factor in equation (15) ranges from 0 to about 1.7, depending on the relative stiffness and thickness of piezoelectric material and substrate. This factor essentially measures the effectiveness of the laminated structure. It can be shown that for a PZT bimorph it is maximum when the substrate's stiffness matches the PZT's and the three layers have the same thickness.

The last factor is essentially determined by the piezoelectric properties of the material. The lowest value worth considering here is that for PVDF, for which this last term is approximately 0.01, as calculated from data in [20]. Currently, the highest piezoelectric coupling is found in crystalline PMN-PT, for which the last term can reach 9 (from data given in [21] for PMN-29PT). For more commonly used polycristalline PZT materials, this term ranges between 0.1 and 0.4, as calculated from data given in [22].

Overall, the range of interest for Γ is no larger than between 10^{-4} and 1 ($\Gamma_{PVDF} \approx 8\ 10^{-4}$ and $\Gamma_{PMN-29PT} \approx 0.62$). Within this range, 21 values were selected uniformly spaced on a logarithmic scale.

3.4. The Forcing

The excitation (see (9)) depends on three parameters. J was selected as $3\ 10^{-3}$ (as the model is linear, it is possible to calculate the outcome of different values by simple rescaling). The point of impact was set at 95% of the length: $x_0 = 0.95$. The sharpness was set at $\sigma = \{0.4, 1, 4\}$, to represent sharp, medium and extremely slow impacts, respectively. Recall that the fundamental period of the non-piezoelectric beam is 2π (see Table 1) whereas the total duration of an impact is approximately $6\,\sigma$.

4. Numerical results and discussion

The system in (14) was numerically solved including 5 modes (N=5) within Maple 16 using the `dsolve` command requiring a `listprocedure` output with the options `maxfun`=10^5 and `numeric;`according to standard practice, the order of the system was reduced by defining an accessory set of variables: $s_n = dq_n/dt$. As all results reported in this section are on the dimensionless model, there are no units on any quantity. Solutions were carried out until time 400, corresponding to over 60 periods. Nonetheless, with some values of Γ and τ, it was found that at the end of this time, the energy generation was still significant. Figure 2 identifies the combinations of parameters for which, in the last 5% of time the cumulative energy increased by more than 3% (a diagram for $\sigma = 4$ is not given as energy conversion was always complete). According to the discussion

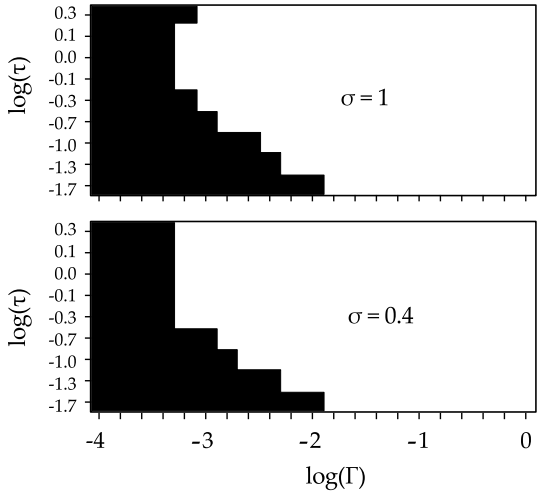

Figure 2. Coloured in black, the combinations of parameters for which the energy $E_c(t)$ increases by more than 3% in the last 5% of time.

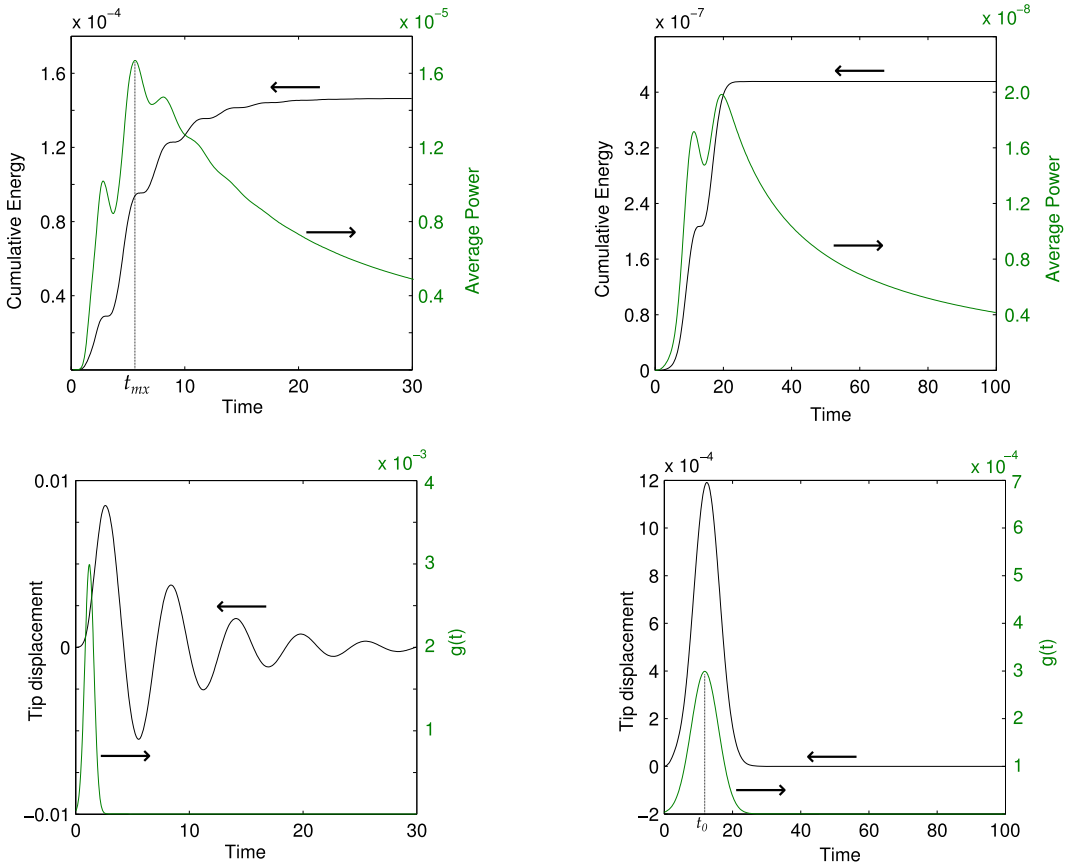

Figure 3. Time evolution of cumulative energy, average power, tip displacement and contact force for two sample runs with $\sigma = 0.4$ (left) and $\sigma = 4$ (right); in both cases $\Gamma = 0.1$ and $\tau = 0.5$.

above, PVDF has $\Gamma \approx 8\ 10^{-4}$, so energy conversion is almost complete if the correct τ is selected.

Time evolution of tip displacement, instantaneous power and cumulative energy are reproduced in figure 3 for two sample runs. A sharp impact ($\sigma = 0.4$) causes the vibration of the bimorph, which progressively dies away as energy is converted or dissipated. If $\sigma = 4$, it is hardly possible to speak of an impact excitation, as the deflection of the bimorph happens synchronously with the forcing and no significant vibrations are induced. Correspondingly, energy generation occurs in two semi-static phases: deflection and relaxation, and it is ≈ 350 times lower than in the first case. These results confirm the advantages of frequency up-conversion, when the bimorph is excited at its resonance frequency. For $\sigma = 1$, the response (not reported here) is similar to that for $\sigma = 0.4$, although with an energy generation ≈ 2.6 times lower. This suggests that, for moderately sharp impacts, the peak contact force is well correlated to the energy generated.

With reference to section 3.1, let us first consider results relevant to the choice of maximising E_c, hence when the EH is designed for sparse impacts. If the impact is sufficiently sharp, the total energy produced is almost independent on the value of Γ (first two graphs in first row in figure 4). For each trace, corresponding to a different value of τ, a maximum is found at intermediate values of Γ.

This discussion suggests that, provided an appropriate τ is selected, any value of Γ will yield roughly the same energy. However, the time required to complete the energy conversion is also likely to be important in applications. The time to achieve 97% of the final energy clearly decreases with increasing Γ (second row in figure 4), with the highest values of τ in general giving the quickest responses, and values around 1 often being optimal. Of practical value is the observation that there is an intermediate range of Γ in which the time drops more quickly, albeit on a semi-log scale.
The quickest conversion for $\sigma = 0.4$ was observed for $\Gamma = 0.63$ and $\tau = 0.2$. It is possible to complete 97% of the conversion within time=16, i.e. less than 3 periods, with $\Gamma > 0.1$ and a suitable choice of τ. In the case of $\sigma = 4$, conversion is completed quickly because, as was previously observed, there are almost no residual vibrations of the bimorph once contact is lost.

A comparative observation of plots in rows 1 and 2 of figure 4 reveals that an optimal choice of energy may not lead to the fastest conversion and vice versa. Ultimately, applications designers aim at maximising overall power output. This task is aided by plots showing the average power generated at the end of the conversion (last row of figure 4). Overall, power is positively correlated with Γ. For any value of Γ, the power is maximised by a particular value of τ; whereas at low Γ a large τ is a fairly safe choice, at high levels of coupling a non-optimal τ brings significant penalties. This observation has important consequences in application, as it suggests that the effort spent to increase Γ (perhaps with expensive piezoelectric materials) can be frustrated by the wrong τ, which in practice can be tuned via the impedance of the power extraction circuit.

Let us now consider the second design scheme discussed previously, intended to maximise the power generated. Interest is in the peak of the curve $P_{av}(t)$ (ref. figure 3). Overall, its value is positively correlated with Γ (first row in figure 5). For each value of

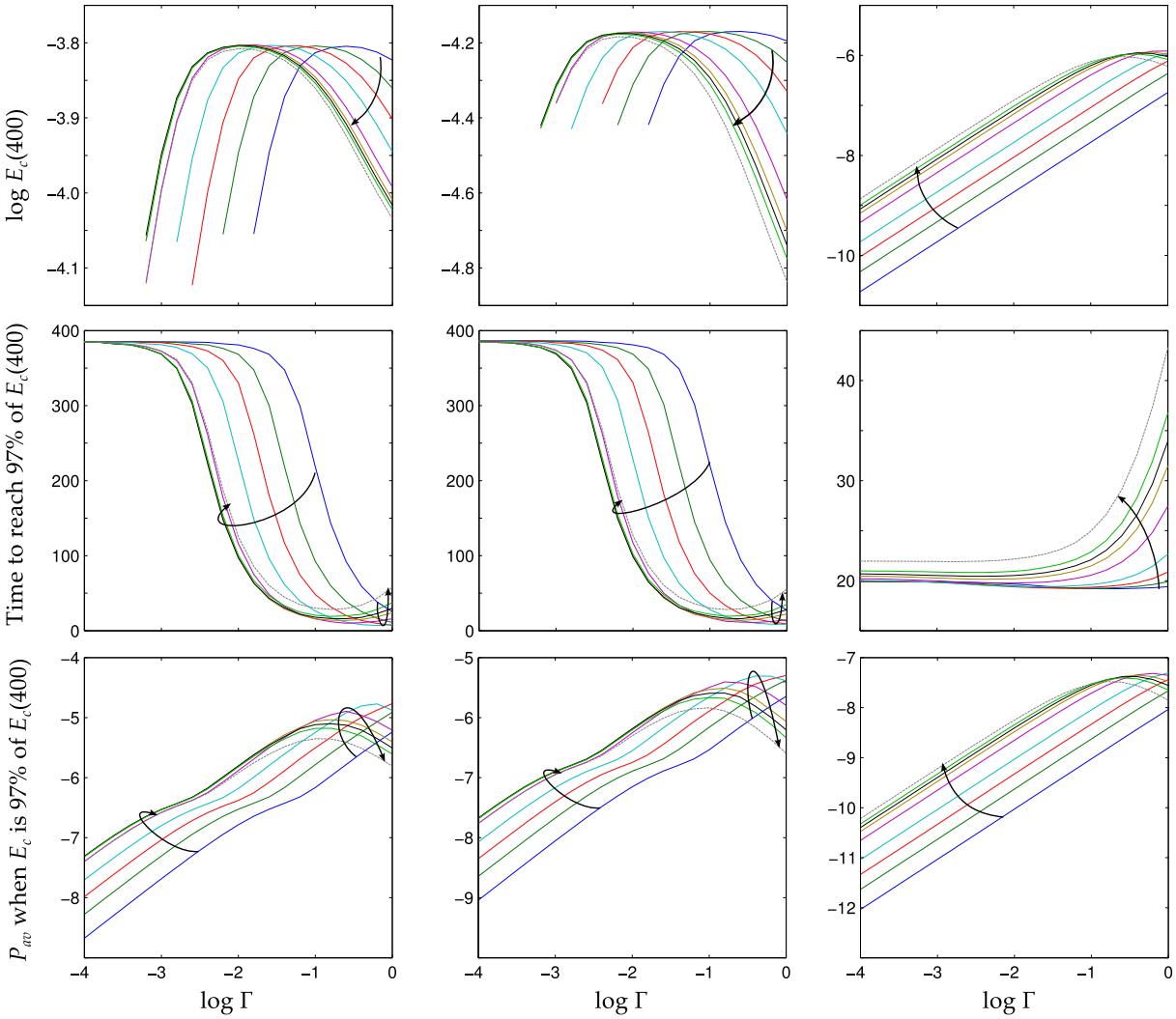

Figure 4. Top→bottom: maximum cumulative energy (value at time=400); time at which generated energy is 97% of the maximum; average power generated in this time. Left→right: $\sigma = 0.4; 1; 4$. The arrows indicate the direction of increasing τ. In the first two graphs, points relating to combinations of parameters for which the energy is still increasing fast are not plotted.

Γ, there is a (decreasing) value of τ which maximises the value of the peak; for $\sigma = 0.4$, an absolute maximum of 2.3 10^{-5} is recorded for $\Gamma = 1$ and $\tau = 0.1$, this is only 33% higher than the maximum power achievable with $\Gamma = 0.1$ and $\tau = 0.5$, i.e. with traditional PZT materials. For each τ, we observe a maximum along Γ, whose cause was already discussed above. A row-wise comparison re-affirms that the power generated is higher for shaper impacts, with a loss of up to almost three orders of magnitude when the "impact" becomes a semi-static deflection.

As discussed previously, the potential power generation presently discussed is attainable only if impacts are repeated with the appropriate frequency. For sharp impacts (first two graphs, second row in figure 5) t_{mx}, i.e. the time position of the peaks in P_{av}, is negatively correlated with Γ: higher Γ in general yield higher power,

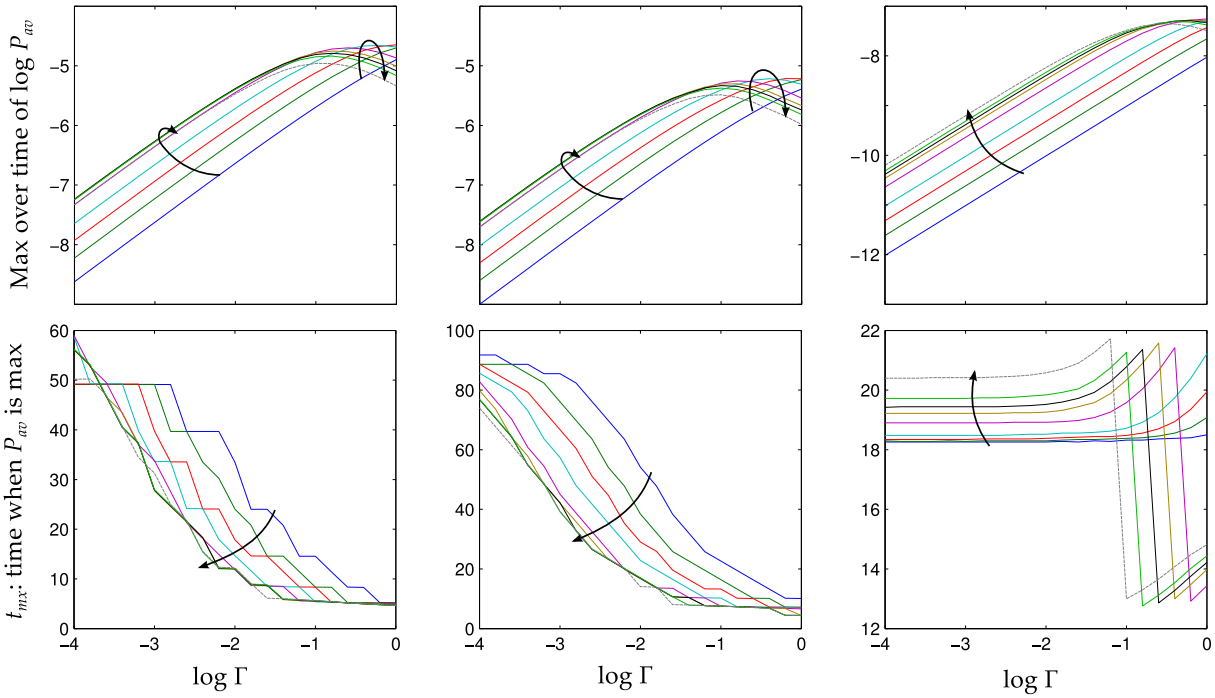

Figure 5. Top →bottom: the logarithm of the maximum over time of P_{av}; the position of said maximum . Left →right: $\sigma = 0.4; 1; 4$. The arrows indicate the direction of increasing τ.

but at the expense of requiring a higher impact frequency. In fact, observing the graphs column-wise it is noted that the highest power outputs correspond to times of 5 to 6, which means one period. This would not be frequency up-conversion any more, as the impact excitation occurs at the same frequency as the fundamental mode of the bimorph.

The step-wise character of the traces in the first two columns is due to the discretisation of the time occurrence of the maximum, dictated by the oscillatory response; the exact value depends on Γ as this affects the resonant frequency of the piezoelectric bimorph. When $\sigma = 4$ (last column), t_{mx} is governed by the forcing function, there are no significant vibrations and $P_{av}(t)$ has up to two peaks. For low Γ, the second peak (relaxation) yields more energy; when Γ exceeds a threshold value (dependent on τ), less energy is produced in the second peak and the first (deflection) is where maximum power is observed.

The EH may be designed so that impact takes place on a specific location along the beam. Maximum energy is generated if the impact occurs at the free end (figure 6). As is visible in the figure, this is also the location where maximum energy is transferred from projectile to beam. It is also clear that the energy generated is strictly related to the energy that the projectile is able to deliver. However, the very sharpest impact ($\sigma = 0.04$) excites higher modes to a very large extent and this yields a poorer conversion efficiency ($\eta_0 \stackrel{\text{def}}{=} E_{out}/E_{in}$) because more energy is lost to internal damping, which increases with frequency. Furthermore, modes above $n = 1$ have inflection points, which

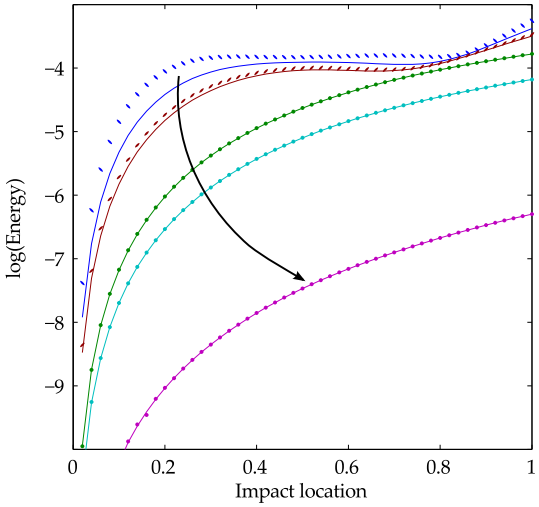

Figure 6. Effect of the impact location on the energy transferred by the projectile (symbols) and the final energy generated (continuous lines) for σ=0.04, 0.1, 0.4, 1 and 4; for all curves, $\Gamma = 0.1$ and $\tau = 0.5$. Coordinate 0 represents the root of the beam, 1 is the free end. Values of σ increase along the arrow.

means that different sections along the beam will generate opposing charges that cannot be extracted. Despite this, as the piezoelectric effect couples the vibrational modes of the beam, energy from higher modes will go to the lower mode to be converted. Analysis of the data in figure 6 relative to $\sigma = 0.04$ reveals that the efficiency is 43% and 75% for impacts at locations 0.2 and 1, respectively; these increase to 81% and 94% for $\sigma = 0.1$ in the same locations. In terms of efficiency, location 0.88 results in an optimal choice, as $\eta_0 \geq 96\%$, for all impacts considered.

In principle, an improvement in conversion efficiency would derive from the use of segmented electrodes, as already proposed for vibrational EH by other researchers [23]. The benefit is related to a quicker extraction of energy, and so less time for dissipation via internal damping. In practical terms, every independent electrode requires, in the simplest case, a dedicated rectifying bridge, which introduces additional complexity and a fixed voltage drop, whose effect on efficiency will depend on the scale of the device.

For the sharpest impacts ($\sigma = 0.04$ and 0.1) local minima are noticed at 0.72 and 0.66, respectively, and local maxima at 0.52 and 0.54 – although the maxima are only 5% above the minima. A similar result was reported by Jacquelin et al.[14] for their *transient* response, which reflects the situation investigated here (in their steady-state response the maximum is global, likely because at steady-state the location of impact affects the speed of the projectile).

As is well known, although not always fully appreciated in its consequences, the stiffness of a piezoelectric material is affected by the external circuit between its electrodes. In particular, a low external resistance yields a more compliant bimorph than a high resistance. This fact can be turned to advantage in impulse-excitation: if the external impedance is switched from ≈ 0 to optimal at an appropriate time during

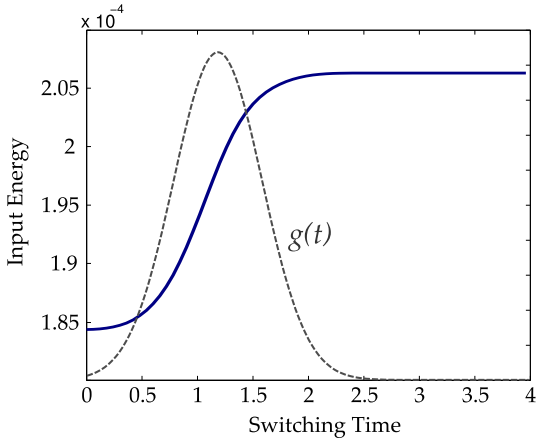

Figure 7. Input mechanical energy as a function of switching time, i.e. when τ is stepped from 0.001 to 0.5. The other parameters were: $\sigma = 0.4$ and $\Gamma = 0.1$. In this specific case, a gain of 12% is observed in the energy available for conversion. The contact force $g(t)$ is also shown (without vertical scale).

or after the impact, the energy generated may be increased. This is because a low stiffness bimorph will receive more energy from the impact than a stiff one (the impact is more inelastic). It is not the intention of this paper to explore this in detail, but to prove the point the model was run with $\tau(t) = \tau_\infty \mathcal{H}(t - t_{sw}) + 0.001$ where $\mathcal{H}$ is the Heaviside step-function, $\sigma = 0.4, \Gamma = 0.1, \tau_\infty = 0.5, t_{sw} \in [0, 4]$. The input mechanical energy (work done by the projectile) was calculated as:

$$W = k_1^4 \int_0^{6\sigma} g(t)\, v(\xi_0, t)\, dt$$

where $v(\xi_0, t)$ is the velocity of the point where the force $g(t)$ is applied.

As predicted, the input energy is higher the longer the external resistance (the only factor in τ assumed to change) is kept low; saturation is observed beyond the loss of contact (figure 7). As τ also affects the ability of the external circuit to extract energy from the bimorph, it remains to be investigated what switching time and what τ_∞ are best matched to give a maximum in energy output.

5. Conclusions

This paper has presented a dimensionless model for piezoelectric energy harvesters, based on an analytical derivation from standard piezoelectricity and Euler-Bernoulli beam theory. The *dimensionless* formulation permits the derivation of results widely applicable, irrespective of the specific materials or geometric dimensions.

The model has been solved with a forcing function representing an impact excitation, which is an increasingly common way to achieve frequency up-conversion, and thence to improve the performance of the EH. Due to the dimensionless character of the model, the results found have general applicability:

- sharper impacts, in which the projectile's momentum is transferred in a very short time, yield higher energy generation. This conclusion is valid within the time-scale investigated, whereas different results may be expected if the impact could be extremely fast and excite much higher modes of vibration, as suggested by figure 6. As such impacts may seriously damage the bimorph, they are of limited interest;
- the final energy generated depends only marginally on the coupling Γ. This is a very important result as it implies that moderately piezoelectric materials may give almost the same energy conversion as more active ones;
- from the energy generation point of view, the major effect of strong coupling (large Γ) is on the time required to achieve the desired energy output. In other words, the highest power outputs can only be achieved when Γ is large;
- combining the latter two points, it is noted that damping becomes more important with small coupling, as the longer is the conversion the more energy will be dissipated. This would be particularly important for polymer-based bimorphs, due to the large internal damping expected. If this case is of interest, further analysis should be done with higher values of damping than was used here;
- the projectile should impact the bimorph close to the free end so as to transfer the maximum energy. The conversion efficiency may depend on the location of impact (figure 6).

Some impulse-excited EHs will require the projectile to preserve a significant proportion of its kinetic energy through the impact, for example to promptly travel to another element where it receives further energy itself. Other EHs may perform best if in the impact the projectile loses as much of its energy as possible. In the latter case, it may be beneficial to initially set the external circuit to low impedance so that the bimorph is more compliant and offers a more inelastic impact; thereafter, the circuit is switched to an optimised impedance, to extract the electrical energy as quickly as possible. This consideration should fit within a global strategy to optimise the impact, for which task it may be useful to refer to [15].

As a general consideration, frequency up-conversion is useful when only a moderate piezoelectric coupling is available, as in this case many vibrations are needed to complete the conversion between input mechanical energy and output electrical energy. When coupling is strong, on the other hand, conversion is quick and after a few periods there is no mechanical energy left in the bimorph. In other words, if the application offers sparse excitations, and in virtue of this it demands frequency up-conversion, then there is no advantage in introducing a bimorph with high coupling. As this may well be associated with exotic materials or geometries, it can be seen as a useless cost. All this has a positive aspect: there are likely to be many applications where the cost of efficient bimorphs would make piezoelectric EH economically infeasible. The results presented in this paper show that frequency up-conversion with unsophisticated bimorphs could be a viable solution in all these cases. The way to higher output power from impact-excited

EHs seems to be paved of many medium quality bimorphs, rather than a few better performing ones.

References

[1] Pozzi M and Zhu M 2011 Plucked piezoelectric bimorphs for knee-joint energy harvesting: modelling and experimental validation *Smart Mater. Struct.* **20** 055007

[2] Kulah H and Najafi K 2004 An electromagnetic micro power generator for low-frequency environmental vibrations *Micro Electro Mechanical Systems, 2004. 17th IEEE International Conference on. (MEMS)* (IEEE) pp 237– 240

[3] Umeda M, Nakamura K and Ueha S 1996 Analysis of the Transformation of Mechanical Impact Energy to Electric Energy Using Piezoelectric Vibrator *Jpn. J. Appl. Phys.* **35** 3267–73

[4] Kulah H and Najafi K 2008 Energy Scavenging From Low-Frequency Vibrations by Using Frequency Up-Conversion for Wireless Sensor Applications *IEEE Sensors Journal* **8** 261–8

[5] Rastegar J and Murray R 2010 Novel two-stage piezoelectric-based electrical energy generators for low and variable speed rotary machinery Active and Passive Smart Structures and Integrated Systems 2010 (San Diego, CA, USA) p 76430C–76430C–8

[6] Pozzi M and Zhu M 2012 Characterization of a rotary piezoelectric energy harvester based on plucking excitation for knee-joint wearable applications *Smart Materials and Structures* **21** 055004

[7] Murray R and Rastegar J 2009 Novel two-stage piezoelectric-based ocean wave energy harvesters for moored or unmoored buoys *Proceedings of SPIE* Active and Passive Smart Structures and Integrated Systems 2009 (San Diego, CA, USA) p 72880E–72880E–12

[8] Pozzi M, Aung M S H, Zhu M, Jones R K and Goulermas J Y 2012 The pizzicato knee-joint energy harvester: characterization with biomechanical data and the effect of backpack load *Smart Mater. Struct.* **21** 075023

[9] Renaud M, Fiorini P, van Schaijk R and van Hoof C 2009 Harvesting energy from the motion of human limbs: the design and analysis of an impact-based piezoelectric generator *Smart Mater. Struct.* **18** 035001

[10] Cavallier B, Berthelot P, Nouira H, Foltete E, Hirsinger L and Ballandras S 2005 Energy harvesting using vibrating structures excited by shock *Ultrasonics Symposium, 2005 IEEE* Ultrasonics Symposium, 2005 IEEE vol 2 pp 943–5

[11] Liu H, Lee C, Kobayashi T, Tay C J and Quan C 2012 Piezoelectric MEMS-based wideband energy harvesting systems using a frequency-up-conversion cantilever stopper *Sensors and Actuators A: Physical* **186** 242–8

[12] Le C P, Halvorsen E, Søråsen O and Yeatman E M 2013 Wideband excitation of an electrostatic vibration energy harvester with power-extracting end-stops *Smart Mater. Struct.* **22** 075020

[13] Gu L and Livermore C 2012 Compact passively self-tuning energy harvesting for rotating applications *Smart Materials and Structures* **21** 015002

[14] Jacquelin E, Adhikari S and Friswell M I 2011 A piezoelectric device for impact energy harvesting *Smart Materials and Structures* **20** 105008

[15] Pashah S, Massenzio M and Jacquelin E 2008 Structural response of impacted structure described through anti-oscillators *International Journal of Impact Engineering* **35** 471–86

[16] Ferrari V and Gatti P L 1999 *Applied Structural and Mechanical Vibrations: Theory, Methods and Measuring Instrumentation* (UK: Spon Pr)

[17] Erturk A and Inman D J 2008 A Distributed Parameter Electromechanical Model for Cantilevered Piezoelectric Energy Harvesters *J. Vib. Acoust.* **130** 041002–15

[18] Anon 1988 IEEE Standard on Piezoelectricity *ANSI/IEEE Std 176-1987*

[19] Han S M, Benaroya H and Wei T 1999 Dynamics of transversely vibrating beams using four engineering theories *Journal of Sound and Vibration* **225** 935–88

[20] Murayama N, Nakamura K, Obara H and Segawa M 1976 The strong piezoelectricity in polyvinylidene fluroide (PVDF) *Ultrasonics* **14** 15–24

[21] Wang F, Luo L, Zhou D, Zhao X and Luo H 2007 Complete set of elastic, dielectric, and piezoelectric constants of orthorhombic 0.71Pb(Mg1/3Nb2/3)O3–0.29PbTiO3 single crystal *Applied Physics Letters* **90** 212903–212903–3

[22] Berlincourt D and Krueger H A 2000 *Properties of Morgan ElectroCeramic Ceramics* (Morgan ElectroCeramics, TP-226)

[23] Erturk A, Tarazaga P A, Farmer J R and Inman D J 2009 Effect of Strain Nodes and Electrode Configuration on Piezoelectric Energy Harvesting From Cantilevered Beams *J. Vib. Acoust.* **131** 011010